Journal of the Serbian Chemical Society
JSCS-info@shd.org.rs • www.shd.org.rs/JSCS
J. Serb. Chem. Soc. 83 (6) 759–772 (2018) UDC 544.4+547.391.3–326:662.61/.62:536.422.4
JSCS–5110 *Original scientific paper*

Kinetics of methyl methacrylate combustion over a Pt/alumina catalyst

IONUT BANU[1], CORINA MIHAELA MANTA[2], IOANA STOICA[1], GEORGETA BERCARU[1] and GRIGORE BOZGA[1]*

[1]*Department of Chemical Engineering and Bioengineering, University Politehnica of Bucharest, 313, Spl. Independentei, Sect. 6, 060042-Bucharest, Romania and* [2]*Sara Pharm Solutions S.R.L., 266-268, Calea Rahovei, Sect. 5, Bucharest, Romania*

(Received 9 August, revised 20 November, accepted 21 December 2017)

Abstract: The combustion of methyl methacrylate (MMA) over a commercial Pt/γ-alumina catalyst was investigated, in the lean air mixtures specific for the depollution applications. The experiments were performed at temperatures between 150 and 360 °C, with MMA concentrations of 460 to 800 ppmv and the gas flow rates between 200 and 300 mL min^{-1}. The results evidenced a negative influence of MMA concentration on the combustion kinetics. A kinetic model of the combustion process was developed, based on the Langmuir–Hinshelwood mechanism, assuming the surface reaction between adsorbed oxygen atoms and adsorbed MMA molecules as the controlling step. The rate expression included the inhibition effects of MMA and water adsorption on the process kinetics. The MMA combustion process simulations evidenced the significant influences of the bulk gas to catalyst particle mass transfer, on the overall kinetics.

Keywords: fixed bed reactor; kinetic model; Langmuir–Hinshelwood; light-off curve; gas–solid mass transfer.

INTRODUCTION

The continuous release of the volatile organic compounds (VOC) into atmosphere has an important impact on the air quality, due to the VOCs intrinsic toxicity, or to their contribution to the formation of photochemical smog.[1]

The methods recommended for the VOCs removal from gaseous effluents depend both on the pollutants nature and on their concentrations. In the case of the gaseous effluents containing low VOC concentration, there are often used the methods based on VOCs combustion. This can be conducted thermally in the absence of catalysts (homogeneous combustion) or in the presence of a solid catalysts (catalytic combustion). The catalytic combustion presents several advent-

* Corresponding author. E-mail: g_bozga@chim.upb.ro
https://doi.org/10.2298/JSC170809008B

ages, compared to the thermal combustion: lower reaction temperature and consequently smaller additional amount of the necessary fuel, the negligible rate of the nitrogen oxidation and the total carbon oxidation to carbon dioxide if the catalyst has an appropriate activity.

Methyl methacrylate (MMA) is an organic compound liquid in normal conditions (n.c.), having the chemical formula $CH_2=C(CH_3)–COOCH_3$, the normal boiling point 384 K, the melting point 225 K, the density (n.c.) 939 kg m^{-3}, the flash point 282 K and the autoignition temperature 708 K.[2] MMA is one of the most important monomers in the polymer industry used in the production of cast acrylic sheets, acrylic emulsions and resins. Data published by the USA Environmental Organization are evidencing that the MMA emissions to air, water and soil, from industries in USA, are approximately 0.46 % of its production.[3] Even if the compound by itself is not likely to cause environmental harm at the levels usually released in the atmosphere, it has an important contribution to the formation of photochemical smog in synergy with other VOCs existent in air (http://www.epa.gov/chemfact/methy-fs.pdf).

Among the materials featuring the catalytic activity for VOC's combustion, the most investigated are the supported noble metals, the supported transitional non-noble metals and the transitional metals oxides.[4–7] So far, the supported noble metal catalysts are the most used in practical applications, as the result of their high activity and the relatively good resistance to deactivation. In this class, the most frequently used are Pt and Pd supported on γ-alumina. The review papers describing VOCs combustion techniques over the supported noble metals catalysts were published by Liotta *et al.*[1] and Diehl *et al.*,[8] respectively. The combustion reactivity of different classes of VOCs on these catalysts, decrease in the order: alcohols > aromatics > ketones > carboxylic acids > alkanes.[8,9]

The performances of the catalysts in VOC combustion are usually evaluated using the VOC conversion–temperature curve (light-off curve), built experimentally at given operating conditions, in continuous laboratory reactors. For the irreversible reactions, such as VOC combustion, the conversion–temperature curve has a sigmoidal shape (S-shape). In the first temperature interval, corresponding to the partial conversion of a reactant, the conversion is strongly increasing with temperature, mainly due to the rate constant increase with temperature. In the higher temperature zone, corresponding to the high conversion values (where the reactant is practically consumed), the curve presents an asymptotical stabilization trend toward the horizontal line corresponding to the total conversion. Duprat[10] examined the possibility to evaluate the apparent reaction order and the limitations of the mass transfer steps from the shape of the light-off curve.

No significant and systematic data were published regarding the mechanism, the kinetics and the relative reactivity for the catalytic combustion in the class of oxygenated compounds. Sawyer and Abraham[11] investigated the oxidation of

ethyl acetate over Pt/γ-alumina catalyst, identifying the small concentrations of ethanol, acetic acid, and diethyl ether, as the intermediary oxidation products. The authors developed the reaction pathways explaining the formation of these partial oxidation products, examining the reaction over the alumina support without Pt. The tests evidenced that Pt has almost exclusively the role of catalyzing the deep oxidation reaction.

Papaefthimiou *et al.*[12,13] showed that ethyl acetate is less reactive than butanol and benzene when they were oxidized over Pt/alumina and Pt/TiO_2 catalysts. The authors found that doping the TiO_2 support with W^{6+} has a positive effect on the activity of Pt catalysts for benzene and ethylacetate oxidation. The proposed ethylacetate oxidation mechanism is assuming that, in a first step, ethylacetate is cracked into smaller organic molecules on the support and that these are subsequently oxidized to CO_2 on the Pt surface. In the case of Pt/TiO_2 (W^{6+}) catalyst, in addition to CO_2, acetic acid is a major byproduct, while acetaldehyde is also formed at low ethylacetate conversions. The presence of acetic acid is explained by its lower oxidation reactivity on Pt, as compared with ethanol and acetaldehyde. Several authors emphasized that, beside the reaction of the molecules adsorbed on the Pt surface, a significant role in the enhancement of the surface reaction kinetics could also play the reaction of the VOC molecules, adsorbed on the alumina support in the proximity of the Pt particles, either by the direct interaction with the adsorbed oxygen, or by a spillover effect.[13–15] Ethylacetate combustion over a CuCeZr/ZSM-5 catalyst was investigated by Li *et al.*[16] The authors reported good activity and stability to the deactivation phenomena of this catalyst, observing that ethanol was the only intermediate product. Mitsui *et al.*[15] studied the acetaldehyde combustion over Pt supported on SnO_2, ZrO_2 and CeO_2. The SnO_2 supported Pt catalysts showed the highest activity, despite low BET surface area. The authors also found that the catalytic activities of ZrO_2 and CeO_2-supported metal catalysts were improved by the reduction treatment in H_2 atmosphere, whereas the catalytic activity of the SnO_2-supported samples was significantly degraded.

The deep oxidation of the short chain alcohols (methanol, ethanol, i-propanol and *n*-propanol) over Au/γ-alumina catalysts was studied by Deng *et al.*[17] The mechanism postulated for methanol combustion assumes that O_2 is firstly activated on the gold cluster and then the activated oxygen spills over the Al_2O_3 surface and reacts with the adsorbed methanol. Depending on the gold concentration, the identified intermediates in the ethanol combustion were acetic acid and acetaldehyde. Good activities for the methanol combustion was evidenced by Cimino *et al.*[18] for a catalyst prepared by Pt electrodeposition on a Fecralloy foam support and by Nair *et al.*,[19] respectively, for a mesoporous $LaMnO_3$ perovskite. For the isopropanol combustion the intermediary product was acetone, whereas for *n*-propanol combustion the formation of propylene and propanal was

observed. In the methyl-isobutyl-ketone (MIBK) the combustion over a Pt/γ-Al_2O_3 catalyst, Tseng *et al.*[20] identified only some trace amounts of acetone and carbon monoxide as the incomplete combustion products. The same authors developed the alternative kinetic models for the MIBK combustion, among which Mars and van Krevelen and Langmuir–Hinshelwood (LH) models were found as most feasible. For the same process, conducted over a Pt/γ-Al_2O_3 catalyst, Banu *et al.*[21] developed a kinetic model based on LH mechanism with the dissociative adsorption of oxygen, and Arzamendi *et al.*[22] proposed a kinetic model based on Mars and van Krevelen mechanism.

Liang and Fang[23] investigated the combustion kinetics of a VOC mixture containing butanone, xylene, toluene, hexane, and benzene over a $La_{0.7}Sr_{0.3}MnO_3$ perovskite-type catalyst. The authors are claiming that the proposed kinetic model predicts the temperature required for the catalytic oxidation of multi- component organic waste gases.

The aim of this work is to investigate the combustion of MMA in the presence of air, over a commercial Pt/alumina catalyst, at low concentrations, specific for the depollution applications. The study brings new data regarding the MMA reactivity and process kinetics. From our best knowledge, there are no studies published so far, regarding the MMA combustion over Pt/alumina catalyst.

EXPERIMENTAL

The liquid methyl methacrylate monomer used in the catalytic combustion study was a high purity product of Merck. As the combustion catalyst we used the commercial 0.5 wt % Pt/γ-alumina ESCAT 26, produced by the former Engelhard company (now BASF) having the main characteristics given in Table I. The commercial pellets of Pt/alumina catalyst were crushed and sieved to particles having the size smaller than 250 μm (average size of 75 μm), which were used in the combustion experiments. The previously published data demonstrated that, for the combustion of other organic compounds having close reactivity with MMA, working with particle size in this interval insures the negligible influence of the internal diffusion on the process kinetics. Ordonez *et al.*[24] found experimentally that the kinetics of the benzene combustion over 0.5wt % Pt/γ-alumina is not influenced by the internal diffusion when the particle size is inferior to 500 μm. Also, the previous research in our group demonstrated that, for the combustion of methyl isobutyl ketone over 0.5wt % Pt/γ-alumina particles smaller than 250 μm, the internal diffusion has a negligible influence on the process kinetics.[25,26]

TABLE I. Pt/alumina catalyst grains characteristics

Pore volume, cm^3/g	0.573
Pore size range, nm	5–25
Average pore diameter, nm	23.6
Specific surface area (BET), m^2/g	97.02
Diameter of catalyst pellet, μm	≤ 250
Density, kg/m^3	650

The combustion reactor consists of a quartz tube having the inner diameter of 4 mm, heated by a controlled electrical furnace. In order to limit the axial temperature gradients, the catalyst was diluted with the inert beads of quartz (0.025 g Pt/γ-alumina and 0.075 g of quartz beads). To monitor the reaction temperature, we used a Pt/Rh thermocouple (approximately 1 mm outer diameter), positioned in the middle of the catalyst bed. The air-MMA vapour mixture was generated bubbling a stream of dried air through a vessel containing the liquid MMA, placed in a thermo-regulated bath. The input MMA concentration was attuned by the bath temperature and by the dilution with a second air stream, by-passing the bubbling vessel. The air flow rates were controlled by the electronic mass flow regulators.

The reaction mixture composition at the reactor outlet was measured by an on-line gas chromatograph (Varian CP-3800 GC with methanizer, Flame Ionization Detector and Thermal Conductivity Detector), provided with a 5 Å molecular sieve column for N_2, O_2, CO, CH_4 and a Hayesep Q column respectively for CO_2 analysis. The calibration of the chromatograph for the carbon oxides was performed by an etalon gaseous mixture provided by Linde Group, whereas for MMA concentration the calibration was based on the measured carbon dioxide concentration resulting from total MMA combustion. Further details regarding the experimental procedure are given by Bosomoiu *et al.*[26] and Manta *et al.*[27,28]

The calculation of MMA conversion was based on both the MMA and CO_2 concentrations measurements at the inlet and the outlet of the reactor respectively. Periodical measurements of MMA conversion, in the identical working conditions, have not evidenced a significant catalyst deactivation during the experimental tests. As oxidation products, beside carbon dioxide, only the negligible concentrations of carbon monoxide were detected, so that the total combustion selectivity to carbon dioxide was found in all experiments. The accuracy of the measurements was evaluated from the carbon balance around the reactor, calculated using the measured flow rates and concentrations of carbon compounds respectively. The carbon balance evidenced a maximum error of 8 % for all the experiments.

Catalytic activity tests

Before the combustion tests, the catalyst activity was stabilized passing an air stream at 400 °C, for 24 h, followed by an air stream containing MMA for approximately 20 h, at 300 °C. The preliminary combustion blank tests demonstrated that the reactor internals did not have a significant catalytic activity in the MMA oxidation. The consistency of the experimental data was demonstrated by the duplicate experiments, modifying the temperature both in upward and downward directions. The conversion-temperature experimental points, given in Fig. 1, demonstrate a suitable reproducibility of the MMA conversion measurements.

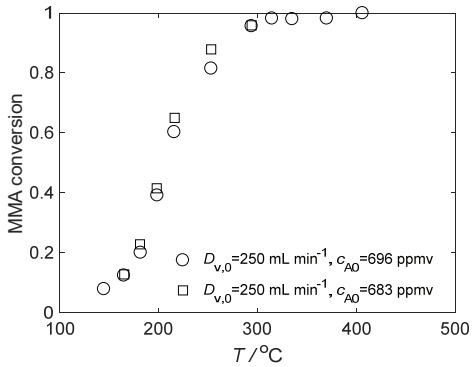

Fig. 1. Tests of conversion measurement reproducibility.

RESULTS AND DISCUSSION

A number of conversion–temperature curves were constructed keeping constant the MMA feed concentration and varying the gas flow rate in the interval 200–300 mL/min. The flow rate interval corresponds to the weight space velocity values, WHSV (mass flow rate to catalyst weight ratios) in the interval 560–850 h^{-1}. As expected, the increase of the flow rate leads to the decrease of MMA conversion, an effect more pronounced on the intermediary conversion and in the temperature interval (Fig. 2). As the observed influence of the gas flow rate on the reactant conversion is relatively low, a limitation effect of the gas to separate the mass-transfer step, from the overall process kinetics, is suspected. Therefore, the influence of this step was included in the process calculations.

The influence of MMA feed concentration on MMA conversion is illustrated in Fig. 3. As observed, the increase of MMA concentration is inducing a decrease of conversion (*e.g.*, a negative reaction order of MMA). The observed negative order kinetics could be explained by the hindering effect, induced by the strong adsorption of MMA molecules, on the oxygen adsorption on the same Pt active centres (favoured by the presence of π-electrons of double bonds and electron doublets of oxygen atoms). This hindrance effect is raised with the increase of the MMA concentration.

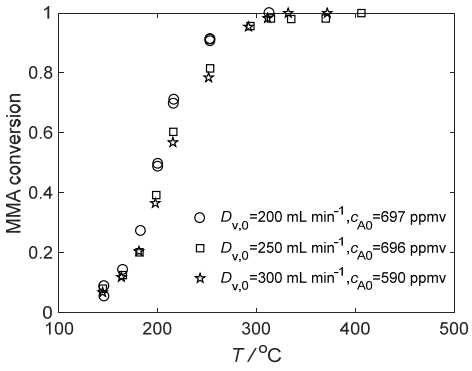

Fig 2. Influence of gas flow rate on MMA conversion (in the legend of the diagram, D_{v0} is the gas flow rate and c_{A0} is MMA feed concentration).

Formulation of a kinetic model for MMA combustion

The MMA combustion stoichiometry is described by the equation:

$$C_3H_5-COOCH_3+6O_2 \xrightarrow{\text{Cat.}} 5CO_2+4H_2O;\ \Delta H_R=-2600\ \text{kJ mol}^{-1} \quad (1)$$

The structure of MMA molecule includes a carbon-carbon double bond, a carbon–oxygen double bond and two oxygen atoms rich in electrons. These characteristics favour the adsorption of MMA molecule on Pt surface. By the analogy with the adsorption of olefins and aromatic rings, it appears plausible to postulate that the adsorbed MMA molecule on Pt consists of π-complexes, oriented in parallel with the metal surface.[8,29] As in olefins oxidation, the next sur-

face step could be the transformation of this π-coordinated MMA-Pt species into di-σ species, followed by the C–C scission and reaction with adsorbed oxygen. The oxygen atoms of carboxylic group are also expected to be adsorbed on Pt surface, forming the species subsequently involved in the surface oxidation of MMA molecule. In parallel, MMA hydrolysis can also occur on the alumina support, giving methanol and acrylic acid. This hypothesis is supported by the findings of Papaefthimiou *et al.*[13] who demonstrated the occurrence of hydrolysis step, during the process of ethyl acetate combustion over Pt/TiO_2 catalyst. The authors postulated that the oxidation of the hydrolysis products occurs in the adsorbed state, mainly on the Pt surface, but also on the support zones near the Pt particles, by the oxygen atoms, migrating from Pt by the spill-over effects.

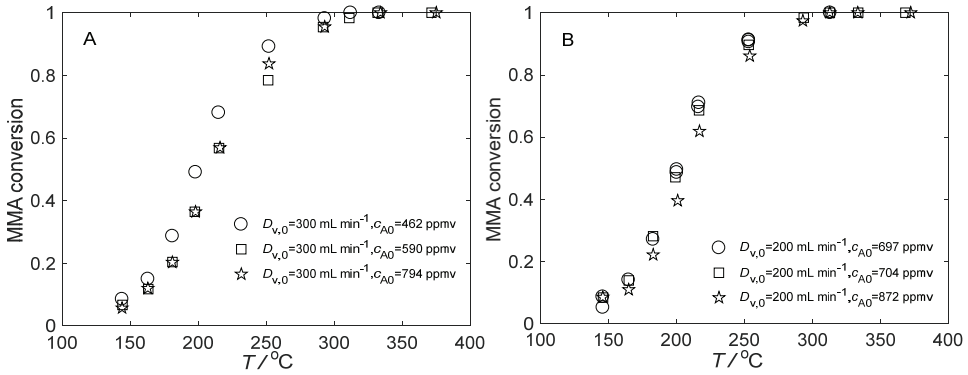

Fig. 3. Influence of feed MMA concentration on the conversion at two gas flow rates: A – 300 mL min^{-1}; B – 200 mL min^{-1} (in the legend of the diagram, D_{v0} is the gas flow rate and c_{A0} is MMA feed concentration).

To deduce a MMA combustion rate expression, the application of the classical LH formalism involves the following steps and equations.[30]

i) The MMA and oxygen adsorption on the active sites, supposed to occur close to equilibrium states (fast steps):

$$\mathrm{A} + \mathrm{X} \overset{K_\mathrm{A}}{\longleftrightarrow} \mathrm{AX}, \; K_\mathrm{A} \cong \frac{\theta_\mathrm{AX}}{p_\mathrm{A}\theta_\mathrm{X}} \tag{2}$$

$$\mathrm{O_2} + 2\,\mathrm{X} \overset{K_\mathrm{O}}{\longleftrightarrow} 2\mathrm{OX}, \; K_\mathrm{O} \cong \frac{\theta_\mathrm{OX}^2}{p_{\mathrm{O_2}}\,\theta_\mathrm{X}^2} \tag{3}$$

ii) Global surface reaction of adsorbed reactants (slow, rate controlling step):

$$\mathrm{A\,X} + 12\;\mathrm{OX} \longrightarrow 5\;\mathrm{PX} + 4\,\mathrm{WX}, \; r_\mathrm{S} = k'\,\theta_\mathrm{AX}\theta_\mathrm{OX} \tag{4}$$

In the above equations, the molecules of MMA, CO_2 and H_2O were denoted by A, P and W respectively. Also, by X and JX are denoted the free active site

and the active site blocked by the adsorption of a molecule or atom J, whereas the fractions of total sites represented by X and JX are denoted by θ_X and θ_{JX}, respectively. K_A and K_O are the adsorption equilibrium constants of MMA and oxygen, respectively.

iii) The products desorption, supposed to occur close to equilibrium is as follows (fast steps):

$$P-X \longleftrightarrow P+X,\ K'_P=\frac{1}{K_P}\cong\frac{p_P\theta_X}{\theta_{PX}} \tag{5}$$

$$W-X \longleftrightarrow W+X,\ K'_W=\frac{1}{K_W}\cong\frac{p_W\theta_X}{\theta_{WX}} \tag{6}$$

K_P and K_W are the adsorption equilibrium constants of CO_2 and water, respectively.

The overall balance of active sites is defined by the equation

$$\theta_X+\theta_{AX}+\theta_{OX}+\theta_{PX}+\theta_{WX}=1 \tag{7}$$

In this equation, the active sites fractions blocked by adsorption have the expressions:

$$\theta_{JX}=K_J p_J \theta_X,\ J=A,P,W \text{ and } \theta_{OX}=\theta_X\sqrt{K_O p_{O_2}} \tag{8}$$

By the combination of the relations (7) and (8):

$$\theta_X=\frac{1}{1+K_A p_A+\sqrt{K_O p_{O_2}}+K_P p_P+K_W p_W} \tag{9}$$

Assuming the overall rate of the surface combustion steps, r_A, equal to the rate of the controlling step, r_S, one obtains:

$$r_A\cong r_S=\frac{k' K_A p_A\sqrt{K_O p_{O_2}}}{(1+K_A p_A+\sqrt{K_O p_{O_2}}+K_P p_P+K_W p_W)^2} \tag{10}$$

The rate constant (k'), and the adsorption equilibrium constants (K_J), are temperature dependent, following the expressions:

$$k'=k'_0\exp\left(-\frac{E'}{RT}\right);\quad K_J=K_{J0}\exp\left(-\frac{\Delta H_{a,J}}{RT}\right);\ J=A,W,O,P \tag{11}$$

E' – activation energy of the surface reaction; $\Delta H_{a,J}$ – adsorption enthalpy change for species J; R –gas constant.

To simplify the kinetic expression and to diminish the number of the unknown parameters, the adsorption terms corresponding to carbon dioxide and oxygen were neglected. Also, considering the high oxygen excess, the partial

pressure of oxygen is assumed constant along the catalyst bed, equal with that in air. In these conditions, the rate expression (10) is simplified to the form:

$$r_A = \frac{k K_A p_A}{(1 + K_A p_A + K_W p_W)^2};\ k = k' K_A \sqrt{K_O p_{O_2}} \tag{12}$$

To diminish the correlation between pre-exponential and exponent parameters, the Arrhenius expressions (11) were used in the equivalent forms:

$$k = k(T_a)\exp\left(\frac{E}{R} z\right);\ K_J = K_J(T_a)\exp\left(\frac{\Delta H_{a,J}}{R} z\right);\ z = \frac{1}{T_a} - \frac{1}{T},\ J = A,W \tag{13}$$

where $E = E' - \Delta H_{a,A} - 0.5\Delta H_{a,O}$ is an apparent activation energy and T_a is the average of working temperatures.

The unknown parameters of the rate expression (12) are $k(T_a)$, $K_A(T_a)$, $K_W(T_a)$, E, $\Delta H_{a,A}$ and $\Delta H_{a,W}$. The estimation of these parameters was done using the function "lsqcurvefit" of the Matlab package. A heterogeneous model, accounting for the interfacial concentration and the temperature gradients and assuming the ideal flow of the gas phase, describes the combustion process in the experimental reactor. The gas phase composition along the catalyst bed was calculated from the MMA balance equation, written in the hypothesis of the gas phase plug flow through the catalyst bed and considering the concentration gradients between the bulk gas and catalyst particle:

$$\frac{d\xi_r}{dm} = \frac{a_v k_G}{\rho_{bed}}(C_A - C_{AS});\ m = 0, \xi_r = 0 \tag{14}$$

ξ_r – the reaction extent; m – mass of catalyst contacted by the reaction mixture; C_A and C_{AS} – gas concentrations of MMA in bulk gas phase and at the surface of catalyst particle respectively; a_v – external particle surface area per unit of catalyst bed volume; k_G – gas to particle mass transfer coefficient; ρ_{bed} – catalyst density in the bed.

The interfacial concentration and temperature gradients were evaluated from heat and mass balance equations around the catalyst particle:

$$a_v k_G (C_A - C_{AS}) = r_A(p_{AS}, T_S)\,\rho_{bed} \tag{15}$$

$$a_v \alpha_h (T_S - T) = (-\Delta H_R)\, r_A(p_{AS}, T_S)\,\rho_{bed} \tag{16}$$

α_h – gas to particle heat transfer coefficient; ΔH_R – reaction enthalpy (heat of reaction).

Eq. (15) represents the condition of equality between the MMA flow rate transferred to the surface of solid catalyst and the transformed rate in the pores of catalyst, reported to the volume unit of catalyst bed. Analogously, Eq. (16) represents the condition of equality between the heat flow rate transferred from

the surface of solid catalyst to the gas phase and the rate of heat generated in the combustion process, reported to the volume unit of catalyst bed.

For the calculation of the gas- particle mass transfer coefficient, we used the relation proposed by Nelson and Galloway[31] for fine particles:

$$Sh = \frac{2\xi + \left\{ \frac{2\xi^2 (1-\varepsilon)^{1/3}}{\left[1-(1-\varepsilon)^{1/3}\right]^2} - 2 \right\} \tanh\xi}{\frac{\xi}{1-(1-\varepsilon)^{1/3}} - \tanh\xi} \; ; \; \xi = 0.3 \left[\frac{1}{(1-\varepsilon)^{1/3}} - 1 \right] \mathrm{Re}^{1/2} \, Sc^{1/3} \quad (17)$$

$$\mathrm{Re} = \frac{u \, \rho_g \, d_p}{\eta_g}; \; Sc = \frac{\eta_g}{\rho_g D_A}; \; Sh = \frac{k_G \, d_p}{D_A}$$

The particle to gas heat transfer coefficient was calculated from the heat and mass transfer analogy involving the following relations:[30]

$$\mathrm{j_D} = \frac{Sh}{Re \; Sc^{1/3}} = \frac{k_G}{u} Sc^{2/3} \quad (18)$$

$$j_H = \frac{\alpha_h}{u \; \rho_g \, c_{pg}} Pr^{2/3}; \; Pr = \frac{\eta_g c_{pg}}{\lambda_g} \quad (19)$$

j_D, j_H – Chilton–Coburn analogy factors for mass and heat respectively; u – superficial gas velocity; ρ_g – gas density; c_{pg} – specific heat of the gas; Pr, Re, Sc, Sh – dimensionless groups of Prandtl, Reynolds, Schmidt and Sherwood, respectively.

The physical properties of the gas mixture were calculated using the data published by Reid *et al.*[32] To limit the distorting influence of the axial temperature gradients, the estimation of the parameters involved in the rate expression (12) was performed using the experimental points corresponding to the MMA conversions smaller than 0.4. These conversion values, obtained over a catalyst diluted in the mass ratio catalyst:inert of 1:3, are supposed not to be significantly influenced by the axial temperature gradients. The calculations revealed that, in the operating region corresponding to the data used in the parameter estimation, the calculated gas-particle concentration gradients are relatively important, particularly at the temperatures above 180 °C, achieving the values up to 9 % reported to bulk gas phase concentration (Fig. 4A). The maximum value of the calculated gas–particle temperature gradient is around 2.5 K, which is at the limit of significance (Fig. 4B).

In Fig. 5A are presented the calculated conversion values *versus* the corresponding experimental ones, on the domain used in the parameter estimation

calculations. The points evidence a good agreement between the calculated and the experimental conversion values, this being a first argument for the adequacy of the proposed kinetic model. Other arguments proving the model quality are the relatively close to the 95 % confidence intervals of the parameter values and a correlation coefficient close to unity (*ro2* = 0.988). The calculated values of the parameters involved in the proposed kinetic model are given in the Table II.

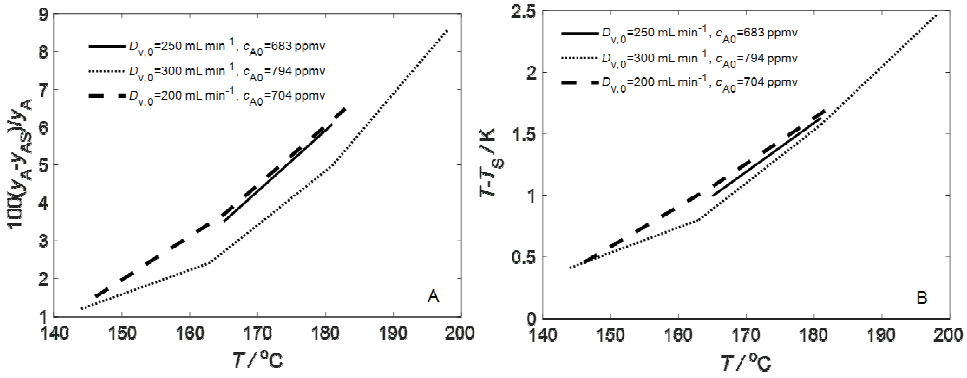

Fig. 4. Gas – particle gradients for MMA concentration (A) and temperature (B) (in the legend of the diagram, D_{v0} is the gas flow rate and c_{A0} is MMA feed concentration).

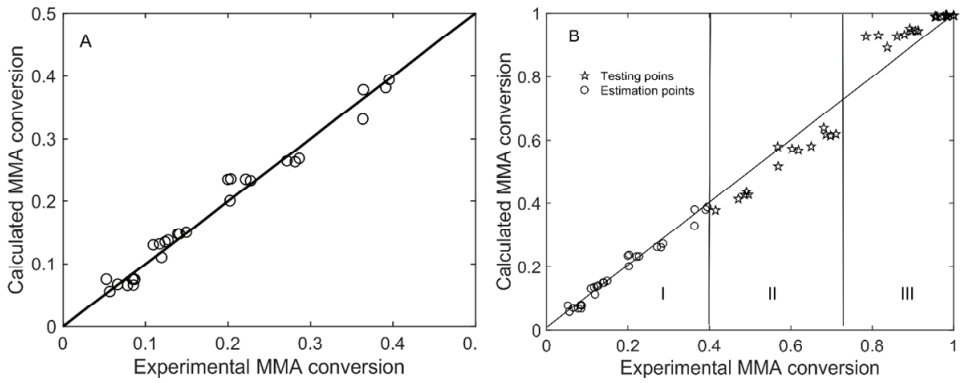

Fig. 5. The parity diagrams: A) estimation domain; B) overall domain.

TABLE II. The estimated parameters for the kinetic model

Parameter	k_0 / kmol kg^{-1} s^{-1}	(E/R) / K	$K_{A,0}$ / bar^{-1}
Value	$6.4607\times10^{9}\cdot(1\pm0.0477)$	$1.2786\times10^{4}\cdot(1\pm0.0337)$	$4.5203\times10^{-3}\cdot(1\pm0.071)$
Parameter	$(\Delta H_{ads,A}/R)$ / K	$K_{W,0}$ / bar^{-1}	$(\Delta H_{ads,W}/R)$ / K
Value	$4.0739\times10^{3}\cdot(1\pm0.0677)$	$7.1186\times10^{-2}\cdot(1\pm0.0363)$	$5.5954\times10^{3}\cdot(1\pm0.0337)$

Beside the points used in the estimation calculations, there were also the conversion values in all the points shown in previous conversion–temperature

diagrams, calculated and compared with experimental data. These comparisons are showed in the parity diagram shown in Fig. 5B.

This diagram can be separated in three domains. The first domain (I) is including the conversion points involved in the estimation calculations, whereas the second (II) and the third (III) domain contain the experimental points corresponding to higher conversions, not considered in the parameter estimation. As observed, in the points of the intermediary domain (II), the calculated MMA conversion is predominantly beneath the measured one. This result can be explained by the average temperature in the bed, slightly superior to the one used in the calculations, as the result of the axial temperature gradients developed in the catalyst bed. Nevertheless, on the domain of highest conversions (III), the calculated values of MMA conversion are higher than the measured ones. This can be explained by more important mass transport limitations occurring in experimental combustion at these temperatures, particularly due to the internal diffusion.

CONCLUSION

This study evidenced that, for the feed concentrations typical for the depollution applications, the complete MMA combustion over 0.5 wt. % Pt/γ-alumina, diluted with the inert beads of quartz in the wt ratio 1:3, is achieved at temperatures above 300 °C, for the weight space velocity values (WHSV) in the interval 560 to 850 h^{-1} and the concentrations between 400 and 800 ppmv. The kinetic study evidenced a surface combustion mechanism obeying the Langmuir–Hinshelwood theory, which involves a surface reaction between the adsorbed MMA molecules and the adsorbed oxygen atoms on the similar active sites. A stronger adsorption of MMA molecules, hindering oxygen adsorption, is explaining the negative apparent reaction order in respect to MMA. The laboratory reactor simulations performed over the entire range of the conversion values confirmed, by comparison with the experimental data, the adequacy of the proposed kinetic model.

Acknowledgement. The work has been funded by the Sectoral Operational Programme Human Resources Development 2007–2013 of the Ministry of European Funds (Romania) through the Financial Agreement POSDRU/159/1.5/S/132395.

ИЗВОД

КИНЕТИКА САГОРЕВАЊА МЕТИЛМЕТАКРИЛАТА НА Pt/ГЛИНИЦА КАТАЛИЗАТОРУ

IONUT BANU[1], CORINA MIHAELA MANTA[2], IOANA STOICA[1], GEORGETA BERCARU[1] и GRIGORE BOZGA[1]

[1]*Department of Chemical Engineering and Bioengineering, University Politehnica of Bucharest, 313, Spl. Independentei, Sect. 6, 060042-Bucharest, Romania and* [2]*Sara Pharm Solutions S.R.L., 266-268, Calea Rahovei, Sect. 5, Bucharest, Romania*

Сагоревање метилметакрилата (ММА) на комерцијалном катализатору, који се састоји од платине и глинице, испитивано је на температурама између 150 и 360 °C, са концентрацијом ММА од 460 до 800 ppmv и са протоком гаса од 200 и300 mL min^{-1}.

Резултати показују негативан утицај концентрације ММА на кинетику сагоревања. Кинетички модел сагоревања је заснован на механизму Ленгмира и Хиншелвуда (Langmuir–Hinshelwood), који претпоставља да је реакција између адсорбованог кисеоника и адсорбованог ММА на површини катализатора спори ступањ реакције. Израз за брзину обухвата ефекте инхибиције ММА и адсорпције воде на кинетику процеса.

(Примљено 9. августа, ревидирано 20. новембра, прихваћено 21. децембра 2017)

REFERENCES

1. L. F. Liotta, *Appl. Catal., B: Environ.* **100** (2010) 403
2. A.W. Gross, J. C. Dobson, in *Kirk-Othmer Encyclopedia of Chemical Technology*, vol. 16, 4th ed., John Wiley & Sons, New York, 1998, pp. 242–245
3. W. Dormer, R. Gomes, M. E. Meek, *Concise International Chemical Assessment Document 4 – Methyl Methacrylate*, World Health Organization, Geneva, 1998
4. F. N. Aguero, M. R. Morales, F. G. Duran, B. P. Barbero, L. E. Cadús, *Chem. Eng. Technol.* **36** (2013) 1749
5. M. Bosomoiu, *PhD Thesis*, University Politehnica of Bucharest, Bucharest, 2008
6. A. O. Rusu, E. Dumitriu, *Environ. Eng. Manage. J.* **2** (2003) 273
7. S. Tanasoi, N. Tanchoux, A. Urda, D. Tichit, I. Sandulescu, F. Fajula, I. C. Marcu, *Appl. Catal., A: Gen.* ***3*63** (2009) 135
8. F. Diehl, J. Barbier jr., D. Duprez, I. Guibard, G. Mabilon, *Appl. Catal., B: Environ.* **95** (2010) 217
9. R. Abbasi, L. Wu, S. E. Wanke, R. E. Hayes, *Chem. Eng. Res. Des.* **90** (2012) 1930
10. F. Duprat, *Chem. Eng. Sci.* **57** (2002) 901
11. J. E. Sawyer, M. A. Abraham , *Ind. Eng. Chem. Res.* **33** (1994) 2084
12. P. Papaefthimiou, T. Ioannides, X. E. Verykios, *Appl. Catal., B: Environ.* **13** (1997) 175
13. P. Papaefthimiou, T. Ioannides, X. E. Verykios, *Appl. Catal., B: Environ.* **15** (1998) 75
14. T. F. Garetto, E. Rincón, C. R. Apesteguía, *Appl. Catal., B: Environ.* **48** (2004) 167
15. T. Mitsui, K. Tsutsui, T. Matsui, R. Kikuchi, K. Eguchi, *Appl. Catal., B: Environ.* **78** (2008) 158
16. S. Li, Q. Hao, R. Zhao, D. Liu, H. Duan, B. Dou, *Chem. Eng. J.* **285** (2016) 536
17. Q. Deng, X. M. Li, Z. S. Peng, Y. F. Long, L. M. Xiang, T. J. Cai, *Transact. Nonferrous Met. Soc. China* **20** (2010) 437
18. S.Cimino, A. Gambirasi, L. Lisi, G. Mancino, M. Musiani, L. Vázquez-Gómez, E. Verlato, *Chem. Eng. J.* **285** (2016) 276
19. M. M. Nair, F. Kleitz, S. Kaliaguine, *Chin. J. Catal.* **37** (2016) 32
20. T. K. Tseng, H. Chu, T. H. Ko, L. K. Chuang, *Chemosphere* **61** (2005) 469
21. I. Banu, G. Bercaru, G. Bozga, T. Danciu, *Chem. Eng. Technol.* **39** (2016) 758
22. G. Arzamendi, F. Roberto, R. P. Angel, L. M. Gandía, *Ind. Eng. Chem. Res.* **46** (2007) 9037
23. C.-J. Liang, J.-W. Fang, *Chem. Eng. Sci.* **144** (2016) 101
24. S. Ordonez, L. Bello, H. Sastre, R. Rosal, F. V. Diez, *Appl. Catal. ,B: Environ.* **38** (2002) 139
25. M. Bosomoiu, G. Bozga, D. Berger, C. Matei, *Appl. Catal., B: Environ.* **84** (2008) 758
26. M. Boşomoiu, A. Soare, C. Gheorghiu, G. Bozga, *Environ. Eng. Manage. J.* **7** (2008) 193
27. C. M. Manta, G. Bozga, G. Bercaru, C. S. Bîldea, *Chem. Eng. Technol.* **34** (2011) 1739
28. C. M. Manta, G. Bozga, G. Bercaru, C. S. Bîldea, *Chem. Eng. Technol.* **35** (2012) 2147
29. G. I. Golodets, *Heterogeneous Catalytic Reactions Involving Molecular Oxygen,* Elsevier, Amsterdam, 1983

30. G. F. Froment, K. B. Bischoff, *Chemical Reactor Analysis and Design*, *Series in Chemical Engineering*, 2nd ed., Wiley, New York, 1990, pp. 71, 128
31. P. A. Nelson, T. R. Galloway, *Chem. Eng. Sci.* **30** (1975) l
32. R. C. Reid, J. M. Prausnitz, B. E. Poling, *The Properties of Gases and Liquids*, 4th ed., McGraw-Hill Book Company, New York, 1987, pp. 392, 586.